

Thick Sputtered Tantalum Coatings for High-Temperature Energy Conversion Applications

V. Stelmakh,* D. Peykov, W. Chan, J. Senkevich,
J. D. Joannopoulos, M. Soljačić, and I. Celanovic

Institute for Soldier Nanotechnologies,

Massachusetts Institute of Technology, Cambridge, Massachusetts, USA

(Dated: July 18, 2015)

Abstract

Thick sputtered tantalum (Ta) coatings on Inconel were investigated as a potential replacement for bulk refractory metal substrates used for high-temperature emitters and absorbers in thermophotovoltaic energy conversion applications. In these applications, high-temperature stability and high reflectance of the surface in the infrared wavelength range are critical in order to sustain operational temperatures and reduce losses due to waste heat. The reflectance of the thick sputtered Ta coatings (8 and 30 μm) was characterized with a conformal protective hafnia (HfO_2) layer as-deposited and after one-hour anneals at 700, 900, and 1100°C. To further understand the high-temperature performance of the sputtered Ta coatings, the micro-structural evolution was investigated as a function of annealing temperature. X-ray diffraction was used to analyze the texture and residual stress in the coatings at four reflections (220, 310, 222, and 321), as-deposited and after anneal. No significant changes in roughness, reflectance, or stress were observed. No delamination or cracking occurred, even after annealing the coatings at 1100°C. Overall, the results of this study suggest that the thick Ta coatings are a promising alternative to bulk substrates and pave the way for a relatively low-cost and easily integrated platform for nano-structured devices in high-temperature energy conversion applications.

* stelmakh@mit.edu

I. INTRODUCTION

Thermophotovoltaic (TPV) energy conversion is a solid state energy conversion scheme with no moving parts and low maintenance requirements that allows for scalable energy production with high power density from a variety of energy sources. In TPV systems, thermal radiation from a heat source at high temperature drives a suitable small bandgap photovoltaic cell. The heat can be produced by hydrocarbon combustion, ideal for lightweight, high power density portable power sources [1–4]; by radioisotopes, ideal for space missions and remote missions requiring power sources with long lifetimes and low maintenance [5]; or by solar radiation absorbed by a suitable absorber and converted to heat [6].

Selective emitters enable higher system efficiencies by tailoring the photonic density of states to produce spectrally confined selective emission of light [7–10]. They can be fabricated as 1D, 2D, and 3D photonic crystals (PhCs) as well as metamaterials [11–17]. Microstructured thermal emitters and absorbers have been studied and fabricated on single crystal tungsten (W) bulk substrates [7, 8, 11, 13–15] as well as polycrystalline Ta and Ta-W alloy bulk substrates [10, 18] by etching a periodic pattern into the low-emissivity (i.e., high reflectivity) metallic substrate. Refractory metals, such as Ta and W, are used in high-temperature ($\geq 900^\circ\text{C}$) energy conversion applications due to their high melting temperature, low vapor pressure, and low infrared emissivity.

Bulk Ta substrates, in particular, are used for selective emitters in TPV systems and for selective absorbers in solar energy systems, as well as for low-emissivity insulating coatings in thermoelectric and solid oxide fuel cell systems. However, bulk emitters add weight to the system and must be welded directly onto the heat source, which is made from a different material than the emitter. In the case of combustion TPV, the heat source can be an Inconel microburner and in the case of radioisotope TPV, the heat source can be a platinum-iridium enclosure. These materials are not suitable for PhC fabrication as they are difficult to etch and do not have the required optical properties. A TPV emitter directly integrated into the system in the form of a coating would require less material, potentially decreasing the fabrication and post-fabrication complexity and integration cost, and would reduce parasitic edge radiation from the thickness of the emitter. Using a Ta coating as a functional layer on different substrates, selected and matched to the system's needs, would decouple the requirements of the functional layer and the substrate.

Previously, the optical and thermo-mechanical properties of sputtered tungsten (W) coatings and their evolution at high temperatures were studied as a potential fabrication route for high-temperature nano-structured surfaces [19]. This study revealed that sputtered W layers were a promising approach to a high-temperature, high-reflectance coating for a PhC substrate, if the challenge of delamination at high temperatures could be overcome. In another study, evaporated thin Ta coatings were found to have low film density and high surface roughness, resulting in low reflectance in the near infrared wavelength range, which made them unsuitable as a PhC substrate [20]. Thus, in this study thicker, denser, highly reflective Ta coatings were deposited via ion-assisted DC magnetron sputtering and investigated as a potential substrate for PhC fabrication.

Thick Ta sputtered coatings have been extensively studied over the past few decades. The coatings have been found to contain one or both of two distinct phases: a stable body-centered cubic (BCC) α -Ta phase that has desirable physical properties, and a metastable tetragonal β -Ta phase that transforms to the BCC phase at around 750°C, is brittle, and has a much higher resistivity and lower reflectance than the α -Ta phase [21, 22]. Three aspects—the factors that cause the β phase instead of the stable α phase [21–30], the sputtering parameters on the morphology and residual stresses of the coatings [26, 29–34], and the effects of annealing on the properties of Ta coatings [35]—have all been previously investigated. Generally, these studies have focused on the stability and the properties of the β phase, on relatively moderate temperatures ($\leq 750^\circ\text{C}$), and on low vacuum conditions [36–42]. However, if α -Ta coatings are ultimately to be used as high-temperature ($\geq 900^\circ\text{C}$) thermal emitters, then their ability to withstand high-vacuum high-temperature anneals must be assessed. Moreover, their optical properties (which are known to be significantly affected by sputtering [31–33, 43, 44] and annealing [20]) must also be known. Therefore the present study evaluates the thermal stability and high-temperature properties of thick sputtered Ta coatings in order to gauge their potential for high-temperature energy conversion applications. The coatings were sputtered on Inconel, a readily available low-cost nickel-chromium-based superalloy used in combustion TPV applications.

Overall, the results of this study suggest that the thick Ta coatings are a promising alternative to bulk substrates and will pave the way for a relatively low-cost and easily integrated platform for nano-structured devices in high-temperature energy conversion applications.

II. EXPERIMENTAL METHODS

Tantalum coatings were fabricated via ion-assisted DC magnetron sputtering on Inconel 625 substrates at a deposition temperature of 300°C at 2 kW. Argon (Ar) was used as the sputtering gas and the vacuum chamber pressure was 2 mTorr with a base pressure of 5×10^{-6} Torr. A 40 V bias was applied on the samples and the discharge filament was run at 40 A for the secondary plasma to increase ion bombardment. The thicknesses of the samples were determined by contact profilometry after deposition and found to be 8 and 30 μm via witness coupons. A 20 nm conformal layer of hafnium oxide (HfO_2) was deposited via atomic layer deposition (ALD) at 250°C, using tetrakis dimethylamino hafnium (TDMAH) and water as precursors, to prevent degradation of the coatings at high temperatures [20].

In order to characterize the optical properties as a function of temperature, the samples were annealed at 700, 900, and 1100°C for one hour in a quartz-lined Inconel tube furnace in vacuum (5×10^{-6} Torr base pressure), at a slow heating and cooling rate of 2°C/minute. The reflectance of the Ta samples was obtained experimentally at room temperature and after each annealing run using an automated spectroradiometric measurement system (Gooch & Housego OL750), scanning the wavelength from 1 to 3 μm .

The prepared samples were imaged by atomic force microscopy (AFM), using the Veeco Nanoscope V Dimension 3100, to characterize the surface and roughness of the coatings as-deposited and after each anneal. In order to quantify and compare the roughness of the coating, the average one-dimensional surface roughness R_a and root-mean-square (RMS) roughness R_q were calculated from the AFM images. In addition, the autocorrelation $R(r)$, which measures the correlation of surface heights separated laterally by the distance r , and height-to-height correlation $H(r)$ functions were calculated. The autocorrelation was fitted using the $R(r) = \exp(-(r/\xi)^{2\alpha})$ approximation model where ξ is the lateral correlation length, defined as the value of r at which $R(r)$ decreases to $1/e$ of its original value, and α is the roughness exponent, extracted from the slope of the corresponding height-to-height correlation function analysis [45].

The residual stress of the coatings was determined via X-ray diffraction (XRD) analysis (Rigaku Smartlab) using a $\sin^2 \psi$ methodology [46, 47], as-deposited and after each anneal. After measuring the d -spacing at several sample rotations ψ , the residual stress σ was

TABLE I: X-ray elastic constants of Ta

hkl	S_2 (10^{-6} MPa $^{-1}$)
220	7.022
310	7.852
222	6.591
321	7.022

calculated (under the assumption of a bi-axial stress state in the film) as

$$\sigma = \frac{1}{d_0} \frac{1}{S_2} \frac{\partial d}{\partial \sin^2 \psi} \quad (1)$$

in which d_0 is the stress-free lattice parameter (taken as the lattice parameter at $\psi = 0$), and the partial derivative $\frac{\partial d}{\partial \sin^2 \psi}$ is calculated from a fit of the results. The X-ray elastic constant of Ta is denoted by $S_2 = (1 + \nu)/E$ which depends on the crystallographic plane of interest, and is equivalent to $(1 + \nu)/E$, where ν is Poisson's ratio and E is the elastic modulus. In this work, four Ta diffraction peaks were analyzed ([220], [310], [222], and [321]), and their respective residual stresses were averaged. The values of S_2 for each peak, calculated from single crystal elastic constants [48–52] as the Neerfeld limit (i.e., the average of the Voigt and Reuss limits), are listed in Table I.

The phase and texture of the sputtered Ta coatings were characterized via XRD analysis and compared after different anneal temperatures. The texture of the films was evaluated using pole figure analysis and compared after different anneal temperatures.

III. RESULTS AND DISCUSSION

A. Roughness and Optical Properties

The topographical results, including the roughness, the lateral correlation length ξ , and the roughness exponent α , are shown in Fig. 1. In all cases, no significant change was observed, thereby revealing that neither the height variation, nor the arrangement of this variation, was affected by annealing.

The optical properties of the coatings as-deposited and after annealing in vacuum at different elevated temperatures were characterized. The reflectance of the Ta sputtered

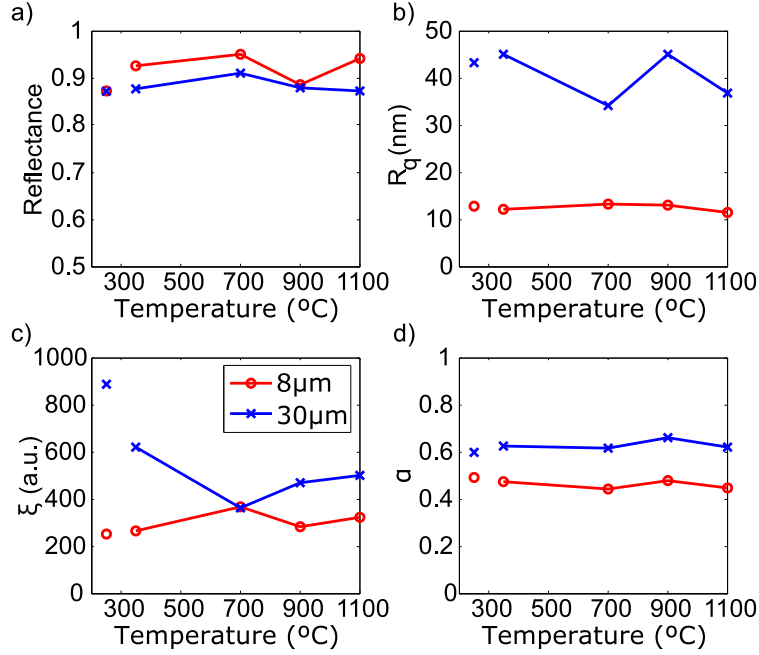


FIG. 1: (Color online) Reflectance measured at 2 μm (a), RMS roughness R_q (b), lateral correlation length ξ (c), and roughness exponent α (d) comparison for the 8 μm and 30 μm coatings as-deposited, as well as after the deposition of the HfO_2 film at 300°C, and after anneal at 700 and 900°C.

coatings was exceptionally high, comparable to that of polished bulk samples. Indeed, dense coatings behave the same as bulk samples, especially in regards to their optical properties [21–23, 33, 34]. The reflectance of the substrates, especially in the IR wavelength range, is of utmost importance, as previously mentioned, for the intended use in energy conversion. Overall, the reflectance of the coatings did not decrease significantly, which was expected since no significant change in roughness was observed, thus meeting the roughness and reflectance requirements for thermal emitters.

B. Phase and Texture

The phase and texture of the sputtered Ta coatings were characterized via X-Ray Diffraction (XRD) analysis. The thick Ta coatings were found to be BCC α -Ta, as shown in Fig. 3. The influence of the deposition conditions—such as sputtering technique, bias voltage, gas, pressure, impurity content, substrate material, substrate temperature, and deposition duration (or thickness)—on the properties of sputtered Ta films has been well studied in the

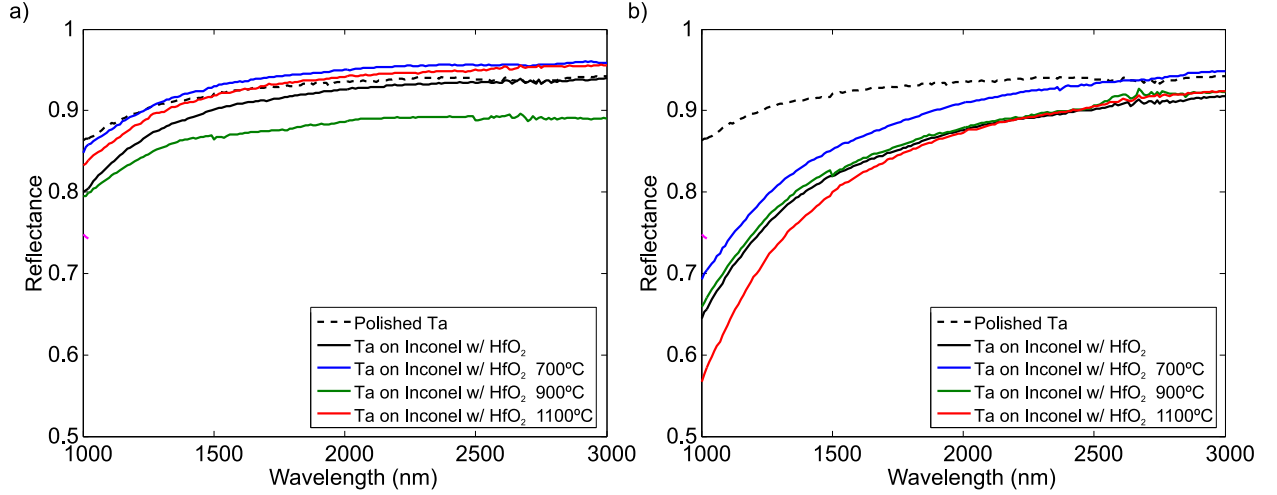


FIG. 2: (Color online) Reflectance of the 8 (a) and 30 μm (b) Ta coating with a protective HfO_2 layer after one-hour anneals at 700, 900, and 1100 $^\circ\text{C}$ compared with flat polished Ta.

All reflectance measurements were made at room temperature.

literature. Depending on the deposition conditions, a different relative amount of β - and α -Ta phase deposit was found. Elevated deposition temperatures promote the formation of BCC α -Ta coatings, whereas lower deposition temperatures lead to β -Ta coatings [24, 28]. The β to α transition temperature was noted as 750-800 $^\circ\text{C}$. In agreement with our findings, previous studies of thick sputtered Ta coatings found the predominant phase to be α -Ta, with increasing β -Ta with decreasing thickness.

From pole figure analysis, a strong (110) fiber texture was observed in both films, as shown in Fig. 4. The (220) surface normals were in the center of the pole figure. The other projections (211) and (200) showed circles, signifying that there is no x and y preference. The (110) direction is relatively dense, and is a common growth direction for BCC films. The pole figures were obtained before anneal and after one-hour anneals at 700 and 900 $^\circ\text{C}$, revealing a fiber texture for all peaks for both coatings at all temperatures.

C. Residual Stress

The calculated residual stress, as defined in Eq. 1 is plotted as a function of the annealing temperature and coating thickness in Figure 5. These results indicate that the as-deposited coatings were highly stressed (values ranging from 1250 to 1750 MPa) and in compression. Values of this magnitude are common for thin films and coatings and have been observed

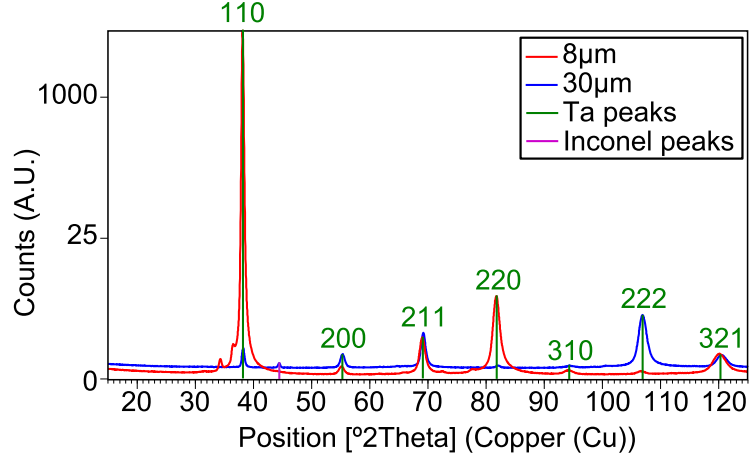


FIG. 3: (Color online) XRD diffraction peaks all originating from α -phase; no β -phase is present. (The small peak to the left of the (110) peak is the Cu β -peak from the instrument).

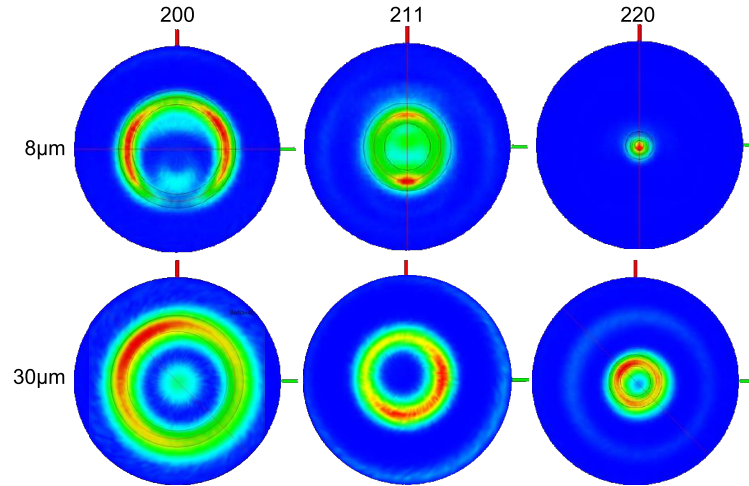


FIG. 4: (Color online) In both films, a strong (110) fiber texture was observed. The (220) surface normals can be seen in the center of the pole figure. The other projections (211) and (200) show circles, signifying that there is no x and y preference.

previously in sputtered Ta samples [27, 29–33, 36, 37, 39–41].

The stress caused by differences in thermal expansion (thermal stress) was calculated, using the thermal expansion data in [53] (assuming that the thickness of the coating is negligible in comparison to that of the substrate) and taking the deposition temperature to be 673 K, and found to be about -800 MPa. The stress caused by the deposition (intrinsic stress) was found to be approximately -450 to -950 MPa. Compressive intrinsic stresses

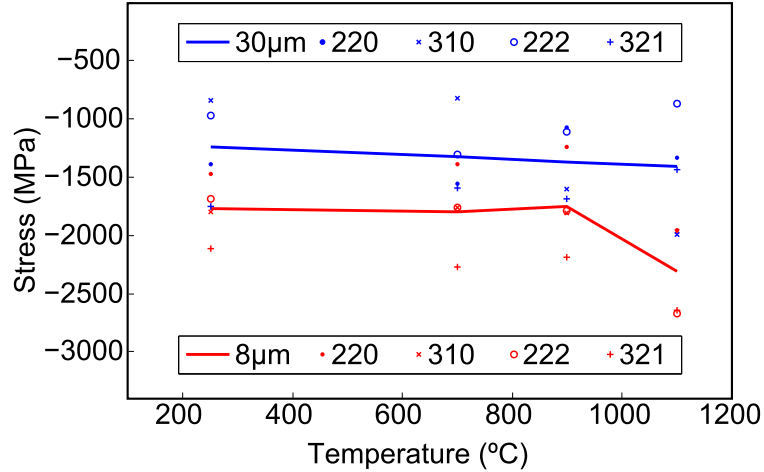


FIG. 5: (Color online) Residual stress of the 8 and 30 μm coatings calculated as-deposited and after anneal at 700, 900, and 1100°C. The line represents the average of the four diffraction peaks considered at each temperature.

are expected in films sputtered with low sputtering pressures, high substrate biases, normal incidence, high target mass, low sputtering gas mass, and a low substrate temperature, as these will produce large particle momenta while maintaining low atomic mobility [43, 44]. As such, Ta coatings deposited with an argon gas (high target to gas mass ratio), at 400°C (low homologous temperature of $0.2T_M$) are expected to be in compression. The occurrence of this intrinsic compressive stress may be beneficial, as it is indicative of dense coatings with optical properties that approach those of bulk materials (i.e., high reflectivity) [31–34, 39, 43, 44]. On the other hand, it is also worth noting that high compressive stresses can lead to coating buckling and poor adhesion.

The change in residual stress after annealing is shown in Fig. 5. For the 30 μm coating, a slight increase in compressive stress with temperature was observed, but all results were well within error of one another. For the 8 μm coating, the residual stress was found to be relatively stable. The only exception was the 1100°C anneal, which caused a sudden increase in compressive stress. However, due to the large scatter in the results from all four diffraction peaks, this increase was not statistically significant. This thermally stable residual stress is in contrast to the previous studies on Ta coatings in which an increase in the compressive stress, increase in the tensile stress, or a reversal from compressive to tensile stress was observed with annealing [36, 37, 40].

The changes in residual stresses with annealing can be attributed to a number of processes:

- Plastic deformation: At high temperatures, the thermal stress may cause the coating to yield, thereby altering the residual stress. However, as the substrate's thermal expansion coefficient is larger than that of the coating, the thermal stresses will tend to decrease the compressive stress, and ultimately produce a net tensile stress on the order of 1500 MPa at 1373 K. This signifies that plastic deformation may be unlikely at the temperatures investigated and with this combination of substrate and coating.
- Phase transformation: Previous work (on β to α transformations [36, 40]) has shown that phase transitions can result in a relaxation of the residual stress. However, as the coatings studied are already in the stable α phase, transformations will not occur.
- Grain growth: At elevated temperatures, the reduction of the grain boundary area of the coating would reduce its excess volume and produce a net tensile stress [43, 44]. However, Ta is unlikely to experience significant grain growth at the temperatures of interest [54–59], and this effect may be negligible.
- Impurities/Oxidation: An increase in the impurity content of the coatings, as well as the formation of tantalum pentoxide (Ta_2O_5), has been associated with an increase in the compressive stress [37–39, 41, 42], which is caused by an associated increase in the volume of the unit cells. However, the protective HfO_2 coating, as well as the high-vacuum conditions, may prevent any significant oxidation, and would therefore prevent volumetric distortion.

IV. CONCLUSION

In TPV applications, bulk PhC substrates add weight to the system and must be integrated with the source of heat which is often made from a different material. An integrated PhC TPV system would require less material, potentially decreasing the fabrication and post-fabrication complexity and integration cost. Using a Ta coating as a functional layer on different substrates, selected and matched to the system's needs, would decouple the requirements of the functional layer and the substrate. In this study we found that the

sputtered Ta layers withstand temperatures up to 1100°C without delamination and can be used as a viable PhC substrate, in contrast to previous studies on W coatings where cracking and delamination occurred.

The reflectance of the Ta sputtered coatings was found to be exceptionally high as-deposited and comparable to that of polished bulk samples. Furthermore, the reflectance of the coatings did not increase significantly after one-hour anneals at temperatures ranging from 700 to 1100°C in vacuum. No significant change in roughness was observed, as expected from the reflectance measurements, thus meeting the roughness and reflectance requirements for thermal emitters. The pole figures, obtained by XRD diffraction before and after the anneals, revealed a fiber texture for all peaks for both coatings at all temperatures. Finally, the Ta sputtered coatings were found to be in a state of compressive stress, thereby producing dense coatings with high reflectivity. Annealing the coatings was not found to produce any significant changes in the residual stress, demonstrating that phenomena such as plastic deformation, phase transformations, grain growth, and oxidation were not significant under these conditions.

Overall, the results of this study suggest that these thick Ta coatings are a promising alternative to bulk substrates as a relatively low-cost and easily integrated platform for nano-structured devices for high-temperature energy conversion applications.

ACKNOWLEDGMENTS

The authors would like to thank: L. Gibbons at H.C. Starck for waterjetting of the inconel substrates; R. Wei, R. Castillo, and K. Coulter at Southwest research Institute for Ta sputtering; J. Guske for assistance with XRD measurements at CMSE (MIT); and V. Rinnerbauer for insightful discussions. ALD was done at CNS at Harvard University, a member of the National Nanotechnology Infrastructure Network (NNIN), supported by the National Science Foundation under NSF Award No. ECS-0335765. Research was supported as part of the Solid-State Solar-Thermal Energy Conversion Center (S3TEC), an Energy Frontier Research Center funded by the U.S. Department of Energy (DOE), Office of Science, Basic Energy Sciences (BES), under Award # DE-SC0001299 / DE-FG02-09ER46577 and by the U.S. Army Research Laboratory and the U.S. Army Research Office through the

- [1] E. Doyle, K. Shukla, and C. Metcalfe, *Development and Demonstration of a 25 Watt Thermophotovoltaic Power Source for a Hybrid Power System*, Tech. Rep. TR04-2001 (National Aeronautics and Space Administration, 2001).
- [2] B. Bitnar, W. Durisch, and R. Holzner, *Appl. Energy* **105**, 430 (2013).
- [3] W. R. Chan, P. Bermel, R. C. N. Pilawa-Podgurski, C. H. Marton, K. F. Jensen, J. J. Senkevich, J. D. Joannopoulos, M. Soljačić, and I. Celanovic, *Proc. Natl. Acad. Sci. U.S.A.* **110**, 5309 (2013).
- [4] W. R. Chan, B. A. Wilhite, J. J. Senkevich, M. Soljačić, J. Joannopoulos, and I. Celanovic, *JPCS* **476**, 012017 (2013).
- [5] C. J. Crowley, N. A. Elkouh, S. Murray, and D. L. Chubb, *AIP Conf. Proc.* **746**, 601 (2005).
- [6] A. Lenert, D. M. Bierman, Y. Nam, W. R. Chan, I. Celanovic, M. Soljačić, and E. N. Wang, *Nat. Nano.* **9**, 126 (2013).
- [7] Y. X. Yeng, M. Ghebrebrhan, P. Bermel, W. R. Chan, J. D. Joannopoulos, M. Soljačić, and I. Celanovic, *Proc. Natl. Acad. Sci. U.S.A.* **109**, 2280 (2012).
- [8] H. Sai, Y. Kanamori, and H. Yugami, *Appl. Phys. Lett.* **82**, 1685 (2003).
- [9] M. Ghebrebrhan, P. Bermel, Y. X. Yeng, I. Celanovic, M. Soljačić, and J. D. Joannopoulos, *Phys. Rev. A* **83**, 033810 (2011).
- [10] V. Rinnerbauer, S. Ndao, Y. X. Yeng, W. R. Chan, J. J. Senkevich, J. D. Joannopoulos, M. Soljačić, and I. Celanovic, *Energy Environ. Sci.* **5**, 8815 (2012).
- [11] A. Heinzl, V. Boerner, A. Gombert, B. Blsi, V. Wittwer, and J. Luther, *J. Mod. Optic.* **47**, 2399 (2000).
- [12] H. Sai and H. Yugami, *Appl. Phys. Lett.* **85**, 3399 (2004).
- [13] E. Rephaeli and S. Fan, *Appl. Phys. Lett.* **92**, 211107 (2008).
- [14] I. Celanovic, N. Jovanovic, and J. Kassakian, *Appl. Phys. Lett.* **92**, 193101 (2008).
- [15] M. Araghchini, Y. X. Yeng, N. Jovanovic, P. Bermel, L. A. Kolodziejski, M. Soljačić, I. Celanovic, and J. D. Joannopoulos, *J. Vac. Sci. Technol. B* **29**, 061402 (2011).
- [16] K. A. Arpin, M. D. Losego, and P. V. Braun, *Chem. of Mater.* **23**, 4783 (2011).
- [17] P. Nagpal, D. Josephson, N. Denny, J. DeWilde, D. Norris, and A. Stein, *J. Mater. Chem.*

- 21**, 10836 (2011).
- [18] V. Stelmakh, V. Rinnerbauer, R. D. Geil, P. R. Aimone, J. J. Senkevich, J. D. Joannopoulos, M. Soljačić, and I. Celanovic, *Appl. Phys. Lett.* **103**, 123903 (2013).
- [19] V. Stelmakh, V. Rinnerbauer, J. D. Joannopoulos, M. Soljačić, I. Celanovic, J. J. Senkevich, C. Tucker, T. Ives, and R. Shrader, *J. Vac. Sci. Technol. A* **31**, 061505 (2013).
- [20] V. Rinnerbauer, J. J. Senkevich, J. D. Joannopoulos, M. Soljačić, I. Celanovic, R. R. Harl, and B. R. Rogers, *J. Vac. Sci. Technol. A* **31**, 011501 (2013).
- [21] D. W. Matson, E. D. McClanahan, J. P. Rice, S. L. Lee, and D. Windover, *Surf. Coat. Technol.* **133–134**, 411 (2000).
- [22] D. W. Matson, E. D. McClanahan, S. L. Lee, and D. Windover, *Surf. Coat. Technol.* **146–147**, 344 (2001).
- [23] W. D. Westwood and F. C. Livermore, *Thin Solid Films* **5**, 407 (1970).
- [24] D. W. Matson, M. D. Merz, and E. D. McClanahan, *J. Vac. Sci. Technol. A* **10**, 1791 (1992).
- [25] R. A. Roy, P. Catania, K. L. Saenger, J. J. Cuomo, and R. L. Lossy, *J. Vac. Sci. Technol. B* **11**, 1921 (1993).
- [26] P. Catania, R. A. Roy, and J. J. Cuomo, *J. Appl. Phys.* **74**, 1008 (1993).
- [27] S. L. Lee and D. Windover, *Surf. Coat. Technol.* **108–109**, 65 (1998).
- [28] S. L. Lee, M. Cipollo, D. Windover, and C. Rickard, *Surf. Coat. Technol.* **120–121**, 44 (1999).
- [29] S. L. Lee, D. Windover, M. Audino, D. W. Matson, and E. D. McClanahan, *Surf. Coat. Technol.* **149**, 62 (2002).
- [30] L. Gladczuk, A. Patel, C. S. Paur, and M. Sosnowski, *Thin Solid Films* **467**, 150 (2004).
- [31] J. A. Thornton and D. W. Hoffman, *J. Vac. Sci. Technol.* **14**, 164 (1977).
- [32] D. W. Hoffman and J. A. Thornton, *J. Vac. Sci. Technol.* **16**, 134 (1979).
- [33] D. W. Hoffman and J. A. Thornton, *J. Vac. Sci. Technol.* **20**, 355 (1982).
- [34] M. Grosser and U. Schmid, *Thin Solid Films* **517**, 4493 (2009).
- [35] V. Rinnerbauer, Y. X. Yeng, W. R. Chan, J. J. Senkevich, J. D. Joannopoulos, M. Soljačić, and I. Celanovic, *Opt. Express* **21**, 11482 (2013).
- [36] L. A. Clevenger, A. Mutscheller, J. M. E. Harper, C. Cabral Jr., and K. Barmak, *J. Appl. Phys.* **72**, 4918 (1992).
- [37] C. Cabral Jr., L. A. Clevenger, and R. G. Schad, *J. Vac. Sci. Technol. B* **12**, 2818 (1994).
- [38] L. Liu, H. Gong, Y. Wang, J. Wang, A. T. S. Wee, and R. Liu, *Mater. Sci. Eng. C* **16**, 85

- (2001).
- [39] B. L. French and J. C. Bilello, *Thin Solid Films* **446**, 91 (2004).
- [40] R. Knepper, K. Jackson, B. Stevens, and S. P. Baker, *MRS Proc.* **854**, U6.8 (2005).
- [41] M. H. Cheng, T. C. Cheng, W. J. Huang, M. N. Chang, and M. K. Chung, *J. Vac. Sci. Technol. B* **25**, 147 (2007).
- [42] D. S. Wu, C. C. Chan, and R. H. Horng, *J. Vac. Sci. Technol. A* **17**, 3327 (1999).
- [43] J. A. Thornton and D. W. Hoffman, *Thin Solid Films* **171**, 5 (1989).
- [44] H. Windischmann, *Crit. Rev. Solid State Mater. Sci.* **17**, 547 (1992).
- [45] M. Pelliccione and T.-M. Lu, *Evolution of Thin Film Morphology: Modeling and Simulations* (Springer-Verlag Berlin Heidelberg, New York, NY, 2008).
- [46] I. C. Noyan and J. B. Cohen, *Mater. Sci. Eng.* **75**, 179 (1985).
- [47] I. C. Noyan, T. C. Huang, and B. R. York, *Crit. Rev. Solid State Mater. Sci.* **20**, 125 (1995).
- [48] G. Simmons and H. Wang, *Single Crystal Elastic Constants and Calculated Aggregate Properties: A Handbook*, 2nd ed. (M.I.T. Press, Cambridge, MA, 1971).
- [49] D. A. Armstrong and B. L. Mordike, *J. Less Common Met.* **22**, 265 (1970).
- [50] R. G. Leisure, D. K. Hsu, and B. A. Seiber, *J. Appl. Phys.* **44**, 3394 (1973).
- [51] W. L. S. III, J. M. Roberts, N. G. Alexandropolous, and K. Salama, *J. Appl. Phys.* **48**, 75 (1977).
- [52] C. E. Anderson and F. R. Brotzen, *J. Appl. Phys.* **53**, 292 (1982).
- [53] Y. S. Touloukian, R. K. Kirby, R. E. Taylor, and P. D. Desai, *Thermophysical Properties of Matter, Volume 12 - Thermal Expansion, Metallic Elements and Alloys* (IFI/Plenum, New York, NY, 1975).
- [54] B. A. Mrowca, *J. Appl. Phys.* **14**, 684 (1943).
- [55] E. M. Savitskii, M. A. Tylkina, and I. A. Tayganova, *Dokl. Akad. Nauk. SSSR* **118**, 720 (1958).
- [56] L. D. Kirkbride, J. A. Basmajian, D. R. Stoller, W. E. Ferguson, R. H. Perkins, and D. N. Dunning, *J. Less Common Met.* **9**, 393 (1965).
- [57] P. Kumar and C. E. Mosheim, *Int. J. Refract. Met. Hard Mater.* **12**, 35 (1993).
- [58] M. F. Hupalo and H. R. Z. Sandim, *Mater. Sci. Eng. A* **318**, 216 (2001).
- [59] S. N. Mathaudhu and K. T. Hartwig, *Mater. Sci. Eng. A* **426**, 128 (2006).